ELSEVIER

Journal of Crystal Growth 222 (2001) 414–425

JOURNAL OF CRYSTAL GROWTH

www.elsevier.nl/locate/jcrysgro

A continuum model for the growth of epitaxial films

Tim P. Schulze[a,*], Weinan E[b,1]

[a] *Department of Mathematics, University of Tennessee, Knoxville, TN 37996-1300, USA*
[b] *Courant Institute of Mathematical Sciences, New York University, 251 Mercer St., New York, NY 10012, USA*

Received 8 June 2000; accepted 10 October 2000
Communicated by D.T.J. Hurle

Abstract

The continuum equations presented here model the growth of epitaxial films in terms of a local edge density $\sim |\nabla h|$ and surface concentration (number density) of adatoms. This model is more amenable to computations than existing models that feature discrete edges and solve continuum equations on each terrace; yet it offers a more detailed picture than continuum models that treat the surface height as the only dependent variable. This latter feature is especially important if one wishes to account for several species which may react on the surface of the film or at step edges to build complicated unit cells. The model is motivated by and compared with numerical solutions of rate equations which are derived from kinetic Monte-Carlo simulations. After introducing the model in a $1+1$ dimensional setting, we extend it to a $2+1$ dimensional setting assuming spatial derivatives become surface gradients. We also discuss extension for the case with multiple species.

1. Introduction

An understanding of the thin-film growth process began with the work of Burton, Cabrera, Frank (BCF) and others who introduced the notion of terrace-step-kink models [1]. In such models, atoms are deposited on the substrate and/or film surface by a variety of techniques (e.g. sputter deposition or chemical vapor deposition), where they wander about before becoming incorporated into the growing crystal lattice. This latter process is most likely to take place at step edges and, more specifically, at kinks in the step edges where the atomic potential favors permanent attachment.

The mathematical modeling and simulation of film growth has taken a variety of approaches, ranging from molecular dynamics and kinetic Monte-Carlo (KMC) simulations to continuum equations that use surface height as the only dependent variable [2]. The former require intense computations and are necessarily limited to very small length scales; the latter offer the promise of revealing larger scale features but are too simple to account for details like surface chemistry. The BCF-like models treat discrete layers of the crystal (the terraces) using continuum equations to track the number density of adatoms on the surface and couple the layers through boundary conditions at

*Corresponding author.
E-mail addresses: schulze@math.utk.edu (T.P. Schulze), weinan@princeton.edu (Weinan E).
[1] Current address. Department of Mathematics and Program in Applied and Computational Mathematics, Princeton University, Princeton, NJ 08544, USA.

0022-0248/01/$ - see front matter
PII: S0022-0248(00)00923-4

the (moving) step edges [1,3]. The step edges themselves are treated as continuous planar curves, though one can incorporate a kink density into such models [4]. These models hold a significant advantage over KPZ [5] and other surface-evolution equations [2] in that one can easily treat multiple species and surface reactions that prefer step edges. Recently, there has been a great deal of computational work on such models using level-set techniques [6–8].

While the latter approach is less computationally demanding than Monte-Carlo simulations, it presents enormously complicated free-boundary problems. The approach we advocate here is a fully continuous model that treats edge density as a surface variable and separately tracks the number density of each adatom species. Like the semi-discrete models just described, this allows one to model multi-species systems and site-specific chemical reactions, but restores the computational ease of the surface evolution equations. Further, we aim to understand in detail the connection between our continuum equations and the MC models, which are presumably more faithful to the microscale physics.

To these ends, we introduce a simple $1+1$ dimensional MC scheme in Section 2. This model is a modified version of the one put forward by Smilaur and Vvedensky [9] that features an explicit adatom surface density. Ultimately, we wish to reproduce the macroscopic consequences of this model. In Section 3 we introduce a new simulation tool, which we term the atomistic difference scheme (ADS). This entails a numerical solution of the rate equations that govern the equilibrium and quasi-equilibrium solutions to the KMC simulations. This method has the advantage of retaining much of the microscale physics, but is much faster than KMC. In Section 4 we solve these same rate equations analytically and consider a continuum limit on the length scale of many terrace widths and time scales comparable to the time it takes a step to advance. This produces a system of coupled differential equations for the homogeneized adatom density and surface height. The continuum equations will incorporate deposition, surface diffusion, Ehrlich–Schwoebel (ES) barriers and adsorption onto step edges. We shall ignore evaporation, desorption, edge diffusion, nucleation and effects due to kinks. In Section 5 we compare the behavior of the ADS and continuum approaches, with the aim of demonstrating the validity of our continuum model. In Section 6 we generalize the model to consider the evolution of films in $2+1$ dimensions and multiple species. We summarize our results and discuss future directions for this research in the final section.

2. Kinetic Monte-Carlo simulations

The principal goal of this work is to find a continuum description of the epitaxial film-growth process that is appropriate for length scales spanning several terraces. Thus, the smallest scale of resolution is larger than that of the BCF approach, which operates on a scale of several lattice spacings. We will, however, retain the BCF formalism that tracks an explicit adatom density $\rho(x)$, which will now be a continuous function of x, the discontinuities at step-edges having been, in some sense, averaged over. While it is possible to homogenize a BCF-type model directly (see the related work of E and Yip [10]) we choose to work here from a more microscopic point of view, with the aim of drawing attention to certain subtleties of the adatom/step-edge interactions.

The MC method described here is based upon the work of Smilaur and Vvedensky and related publications [9], these models having themselves been patterned after earlier simulations performed by Weeks and Gilmer [11]. Like most studies, we focus on single-species cube-on-cube epitaxy, incorporating the basic assumption that atoms arrive onto the surface of the film/substrate in a stochastic manner as the result of some deposition process like pulsed laser deposition, molecular beam epitaxy or chemical vapor deposition. A second assumption is that these surface atoms (commonly referred to as "adatoms") occupy discrete positions on the film or substrate that lie on a regular cubic lattice. We shall ignore nucleation, focusing instead on a "step-flow" problem where we follow the evolution of an initial step configuration.

After landing on the surface of the film/substrate, it is assumed that an isolated atom on an otherwise flat, or "vicinal", surface will be loosely bonded to the film by its attraction to the material below it, but sufficiently energetic to move randomly on the surface with a characteristic "hopping" frequency. This random motion takes the atom from one lattice site to a neighboring site with probabilities calculated from a potential ϕ that depends on the local surface configuration. In $1+1$ dimensions the number of relevant configurations is quite small, it being assumed that there are no overhangs and that the vast majority of steps on the surface are a single unit cell in height. This latter assumption is justified by the slow growth rate of the film which couples with the tendency of atoms to fill in vacancies and attach at existing step-edges before nucleating new layers of growth.

The hopping rate per small, discrete time interval is given by

$$k_i^{\pm} = \tau \exp \frac{\Delta\phi}{k_b \tau},$$

where i is an integer indicating the lattice site, a $+$ or $-$ superscript indicates the direction of the hop, τ is a temperature-dependent hoping frequency, k_b is the Boltzmann constant and $\Delta\phi$ represents the potential barrier to be overcome in the transition from one site to the next (see Fig. 1). The hopping barrier depends on a count of the nearest in- and out-of-plane neighbors. Typically, one assumes there is a deep well at the lower end of each step due to the significant attraction of the in-plane nearest neighbor. The step-edge barrier at the top end of each step is a manifestation of what is known as the Ehrlich–Schwoebel effect [12] and is due to the fact that the last site on each step has one fewer out-of-plane neighbor than the other sites on the terrace. It is recognized [13,14] that this asymmetry in the hopping potential has a significant effect on the dynamics of the film growth. Below we refer to just the symmetric portion of the interstep barrier as "edge" barrier and the asymmetric part as the ES barrier.

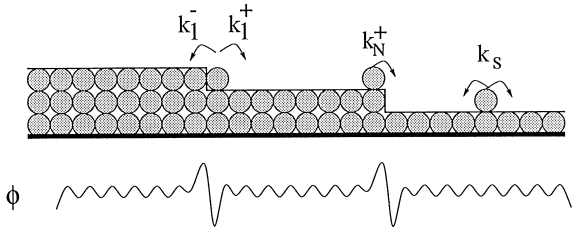

Fig. 1. A schematic drawing of a $1+1$-dimensional epitaxial film illustrating the potential barrier ϕ that determines the hopping rates $k_i^{\pm}$. Most sites have three nearest neighbors in the plane below the adatom, resulting in a generic hopping rate k_s.

These theories can become quite complicated for surfaces, but are greatly simplified – yet well illustrated – in the $1+1$ dimensional case where there are just four rates that need be distinguished: a rate common to all vicinal sites, which we label k_s, the difficult transition over the Schwoebel barrier k_n^+ and away from a step edge k_1^+ and the extremely difficult transition k_1^- that must overcome both of these effects. Note that there are just two independent parameters due to scaling and the "detailed balance" relationship,

$$k_1^+ k_n^+ = k_1^- k_s, \tag{1}$$

that indicates the rates are derived from a continuous potential. From physical considerations, it is clear that the hopping rates satisfy

$$k_s > k_n^+ > k_1^+ > k_1^- \tag{2}$$

with k_1^+ and k_n^+ indicative of the strength of the edge and Schwoebel barriers, respectively.

In typical MC simulations, the only distinction that is made between "adatoms" and atoms which have become embedded in the crystal is that the latter are completely covered and assigned a hopping rate of zero. In the end, only one surface variable, the height of each column of atoms h_i, is kept track of – much like existing continuum models that feature evolution equations for a continuous, macroscopic surface height $h(x)$. This practice is in contrast to the BCF tradition of calculating an adatom density on terraces and coupling this via constitutive laws to free boundaries that represent the moving step edges. The MC model adopted here follows this latter approach by tracking adatom locations on the surface and treating attachment as a separate stochastic process. This is done to present a hierarchy of consistent, inter-related

models – discrete, semi-discrete and continuum – and to derive a continuum model that is readily adapted to multi-species growth, where a distinction between atoms on the surface and reactions to form unit cells must clearly be made. In view of this reasoning, we allow adatom attachment to occur at step edges with a "reaction" rate α.

3. Atomistic difference scheme

MC simulations like those described above are notoriously slow and the results from any given simulation can be difficult to interpret due to the noise in the data. Since we are interested in the average behavior over many terraces, we present an alternative approach here based on numerical solutions of the rate equations that govern the dynamics of the adatom distribution for the MC scheme outlined above. We term this new method an atomistic difference scheme (ADS).

We take ρ_i^j to be the expected number of adatoms at site i at time-step j. This number will be small at most sites and we will ignore interactions between random walkers. In this limit ρ_i^j will be approximately equal to the occupation probability at site i during time interval j. The difference equation corresponding to this process is

$$\frac{\rho_i^{j+1}-\rho_i^j}{\Delta t} = k_{i-1}^+\rho_{i-1}^j - (k_i^- + k_i^+)\rho_i^j + k_{i+1}^-\rho_{i+1}^j - \alpha_i\rho_i^j + F, \tag{3}$$

The coefficients $k_i^\pm$ and α_i depend on the topography of the terraces $\{h_i^j\}$ which varies on a much slower time scale than that of the adatom density. Specifically, the height function evolves according to

$$\frac{h_i^{j+1}-h_i^j}{\Delta t} = \alpha_i\rho_i^j$$

with

$$\alpha_i = \begin{cases} \alpha & \text{at the lower side of a step edge,} \\ 0 & \text{otherwise.} \end{cases}$$

Note that the h_i^j's are real-valued functions despite the discrete nature of the growth process. At each time step a check is made to determine whether enough mass has accumulated at an edge site to form a new unit cell and move the step forward. If this is the case, the coefficients α_i and $k_i^\pm$ are shifted locally by one site. When a step moves it is assumed that the adatom density is not transported with it – i.e. the attachment and hopping rates are advected with the steps but the adatom distribution is not. In other words, the configuration of the surface is defined as the minimum integer-valued piecewise constant approximation to the height function. Note that Δt has to be small enough such that $\Delta t\alpha\rho_i^j < 1$.

If we ignore, for the moment, the motion of the steps, we find that the difference equations (3) admit a stationary and spatially period solution for large times, where $\rho_i^j = \rho_{i+n}^j$, and n is the length of each terrace. This solution is easily found in analytic form or by numerical means.

In Fig. 2 we illustrate solutions for the parameter values $\alpha = 0.01$, $F = 1.0\times10^{-5}$ and a step width of $n = 20$. Fig. 2a features completely homogeneous hopping rates $k_i^\pm = 0.5$. The step spacing can be chosen arbitrarily for $n > 1$ and there is an arbitrary phase factor which positions the steps within the domain. On each step, the adatom density is parabolic and symmetric from left to right. The corresponding step train is linear and descending to the right. In Fig. 2b we use the same parameters with the exception of $k_1^\pm$, which have now been set to 0.01 so that there is a large edge barrier, but no ES barrier. The situation is once again symmetric, but the parabolic adatom distribution on each step is now augmented by a spike in the adatom density at the step edges, due to the attraction of the steps. Finally, in Fig. 2c we use these parameters with the additional change $k_n^+ = 0.05$, corresponding to an intermediate sized ES barrier in addition to the large edge barrier. Now we see that the left–right symmetry on each step has been broken, as adatoms accumulate (on average) at the right end of each step due to the ES barrier.

At each lattice site there is a micro-scale surface current

$$J_i = k_i^+\rho_i - k_{i+1}^-\rho_{i+1} \tag{4}$$

from site i to $i+1$. In all three cases, the equilibrium current is locally linear and periodic.

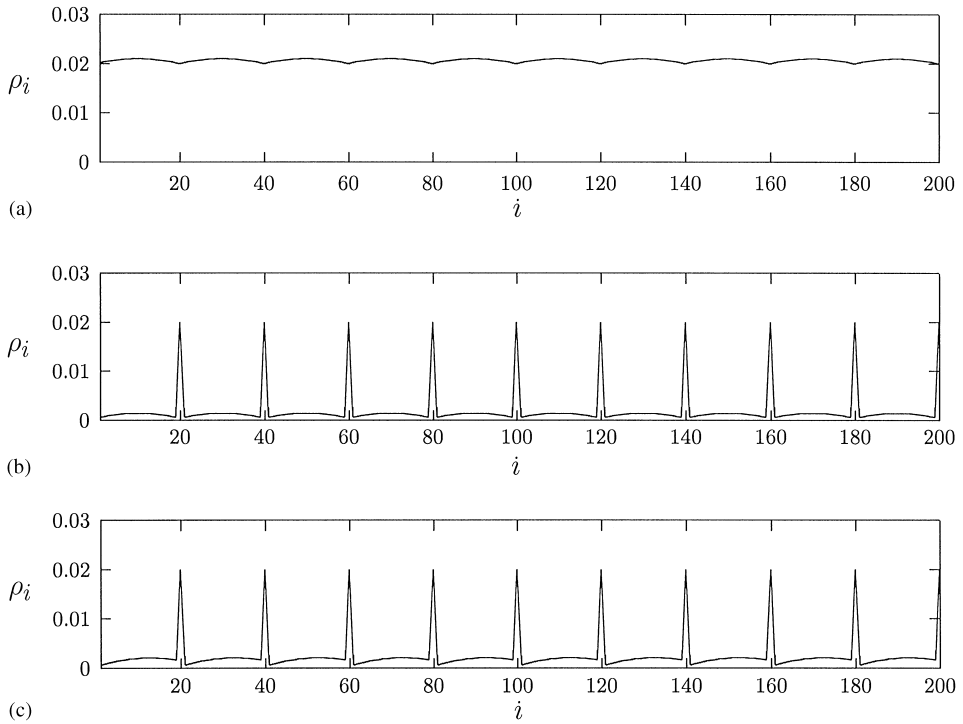

Fig. 2. These three figures illustrate typical equilibrium adatom densities for a periodic step train where (a) all of the hopping rates $k_i^{\pm} = k_s = 0.5$; (b) where there is an edge barrier $k_1^{\pm} \ll k_s$ but no ES barrier $k_n^{+} = k_s$ and (c) where both barriers are present and satisfy $k_1^{-} < k_1^{+} < k_n^{+} < k_s$.

The difference between successive currents on neighboring sites (or "divergence") is given by the source F. At a step edge i, the surface flux from the sites ahead of and behind the step combine with the source to give a sink $\alpha\rho_i$. In the first two cases shown in Fig. 2 the surface current is symmetric in that the same amount of material is supplying the step edge from the front and back, whereas the ES barrier introduces an asymmetry, as is well known. Figs. 3a and b illustrate the local current at each site of a periodic lattice for the case of a symmetric and asymmetric potential.

We shall be especially concerned with such asymmetries or "drifts" in what follows. Note that in equilibrium, the drift in the adatom density is only sufficient to supply the nearest step in the uphill direction – there is no net surface current from one step to the next as a result of the detailed balance relationship (1). We term such a drift "local" and note that it is incapable of transporting adatoms over more than one terrace width. Put another way, the probability of an adatom at site i reaching site $i \pm n$ on an n-periodic step train is exactly the same for the equilibrium solution whether or not an ES barrier is present. Nevertheless, this current has global consequences as it affects the step-width distribution in an asymmetric way that is propagated to neighboring steps.

A second source of asymmetry is introduced into the system by the motion of the steps. When this occurs, non-equilibrium effects can produce global mass transport that is biased in the up- or down-hill directions. To see this, note that immediately after an attachment event has occurred, the adatom distribution is virtually unchanged, but the hopping rates have moved with the step. This is followed by a transient phase where the adatoms reestablish the equilibrium distribution with the new surface configuration. This is illustrated in Fig. 4 where we plot the average surface current

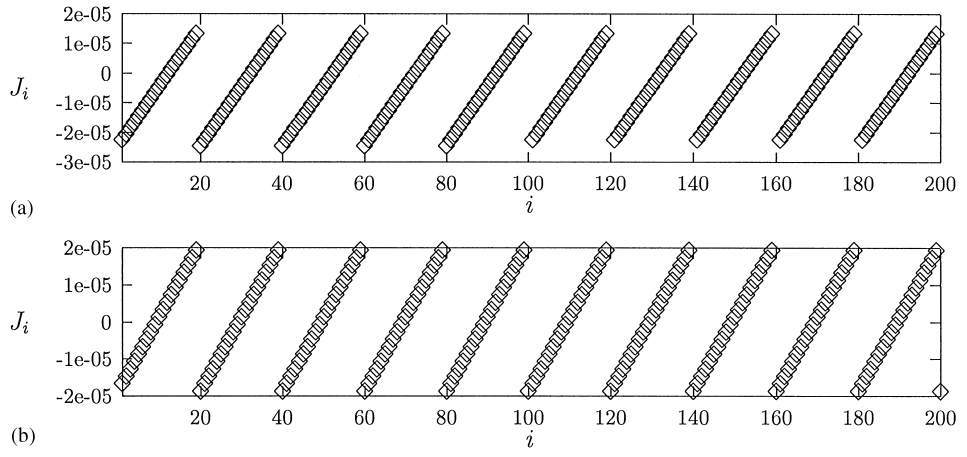

Fig. 3. The local surface current J_i as a function of i for steps with (a) and without (b) an ES barrier. Notice that the current is asymmetric in the first case.

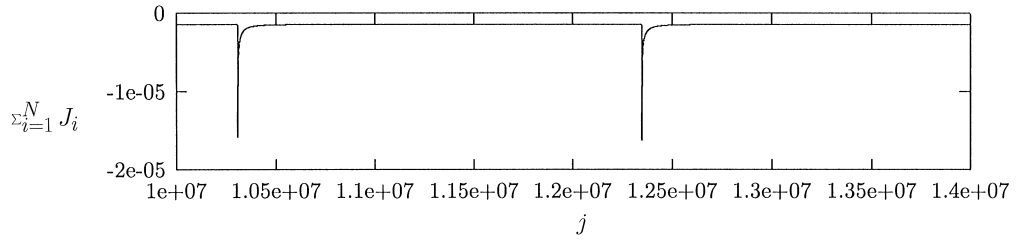

Fig. 4. Surface average of the current as a function of time, revealing the non-equilibrium contribution to the current and fast relaxation time following a step-attachment event.

over one terrace as a function of the time step for the case with an ES barrier.

4. The continuum model

The aim of this section is to present the following model for the step-flow growth of epitaxial thin films

$$\bar{\rho}_t = D\rho_{xx} - S(\rho h_x)_x - \alpha\rho|h_x| + F, \tag{5}$$

$$h_t = \alpha\rho|h_x|, \tag{6}$$

where $\bar{\rho}$ is average adatom density over one terrace width and time scales that are characterized by the time it takes a step to move one site, ρ is the average adatom density at the step edges over the same time scale. The first term on the right-hand side of Eq. (5) is a standard density-gradient-driven diffusion; the second is a drift term which reflects an interaction between adatoms and step edges, the density of which is measured by the surface gradient; the third term represents a sink of adatoms at edge sites, which results in a corresponding source term in the height evolution equation; and the final term is the result of deposition, which we take to be uniform. Below, we outline in a somewhat more detailed way why this equation ought to emerge from the difference equations presented in the previous section.

Eq. (5) follows from conservation of mass once we have derived an expression for the surface current in terms of the macro-scale variables. Since the height and adatom-density rate equations are coupled only at step edges, the adatom density at edge sites provides a convenient and natural measure of the adatom density on the inter-terrace length scale. If we label the density at a particular edge site ρ_1, then the other site we are interested in is ρ_{1+n}, which

will be written as $\rho(x)$ when we take the continuum limit.

To make a direct connection between the ADS approach discussed in the last section and the continuum Eqs. (5) and (6), we will adopt the quasi-static approximation for the rate equation. This amounts to saying that the adatom density on each terrace relaxes quickly to accommodate the change of the surface configuration, which changes rather slowly. The ratio of the two time scales is given by the coverage which will always be assumed small.

On any given time step, the sum of the microscale currents J_i^j averaged over a terrace of length n gives

$$\bar{J}^j = \frac{1}{n}\sum_{i=1}^{n} J_i^j = (k_1^+\rho_1^j - k_n^-\rho_{1+n}^j + k_n^+\rho_n^j - k_s\rho_n^j)/n. \tag{7}$$

Taking Eq. (1) into account, we see that this reduces to

$$k_1^+\frac{(\rho_{1+n}^j - \rho_1^j)}{n}$$

where there is no ES barrier, indicating $D = k_1^+$. For more general values of the hopping rates, we must express the equilibrium value of ρ_n^j as a function of ρ_{1+jn}^j, the edge adatom densities. This will be done by using the steady-state rate equations for a discrete MC process taking place on an arbitrary step of size n:

$$k_{i-1}^+\rho_{i-1} - (k_i^- + k_i^+)\rho_i + k_{i+1}^-\rho_{i+1} - \alpha_i\rho_i + F = 0,$$

where we have dropped the superscript in view of the steady-state assumption. From these equations we must eliminate all of the ρ_i except ρ_1, ρ_n and ρ_{1+n}. To do this, we will need the equations centered at sites 2 through n, the first and last of which are

$$\begin{aligned} &k_1^+\rho_1 - 2k_s\rho_2 + k_s\rho_3 + F = 0,\\ &k_s\rho_{n-1} - (k_n^+ + k_s)\rho_n + k_1^-\rho_{1+n} + F = 0. \end{aligned} \tag{8}$$

The remaining equations are all of the form

$$k_s\rho_{i-1} - 2k_s\rho_i + k_s\rho_{i+1} + F = 0$$

which has the general solution

$$\rho_i = \rho_n + (i-n)B - \frac{F}{2k_s}(i-n)^2. \tag{9}$$

Using this relationship we can eliminate ρ_2, ρ_3 and ρ_{n-1} from Eqs. (8), leaving us with the two unknown quantities ρ_n and B. We then form a linear combination of Eq. (8) to eliminate B and determine a leading order expression for ρ_n. As n becomes large this gives

$$\rho_n = \frac{nF}{2k_n^+} + \frac{k_1^-}{k_n^+}\rho_{1+n}.$$

Now, we substitute this result applied to ρ_{1+n} into Eq. (7) to arrive at

$$\bar{J} = \frac{1}{n}\left[k_1^+\rho_1 - k_1^-\rho_{1+n} + (k_n^+ - k_s)\left(\frac{nF}{2k_n^+} + \frac{k_1^-}{k_n^+}\rho_{1+n}\right)\right]$$

which simplifies to give

$$-\bar{J} = k_1^+\frac{\rho_{n+1} - \rho_1}{n} - \frac{F}{2}\left(\frac{k_s}{k_n^+} - 1\right)$$

the first term being the diffusively driven mass flux and the second accounting for the steady drift.

On a uniform step train, F is approximately related to ρ_{1+n} by

$$\alpha\rho_{1+jn} = nF, \tag{10}$$

where n is the width of the terraces. This is obtained by a simple mass balance and can be combined with the previous result to give

$$-\bar{J} = k_1^+\frac{\rho_{n+1} - \rho_1}{n} + \frac{\alpha\rho_{n+1}}{2n}\left(\frac{k_s}{k_n^+} - 1\right),$$

where we have expressed nF using the adatom density ρ_{1+n}.

In the continuum limit we wish to express the current as

$$-\bar{J} = D\rho_x - S\rho h_x.$$

Noting $h_x < 0$ for our step train, this last result gives the leading order relationships

$$\begin{aligned} &D = k_1^+,\\ &S = \frac{\alpha}{2}\left(\frac{k_s}{k_n^+} - 1\right). \end{aligned} \tag{11}$$

This is our main result.

In order to correctly express the conservation of mass on the film surface, we need to evaluate the average adatom density on the terraces in terms of ρ_{1+nj}. This is easily done using

Eq. (9) and gives

$$\bar{\rho} = \frac{k_1^-}{k_n^+}\rho + \frac{F}{12k_s}\frac{1}{h_x^2}. \tag{12}$$

Finally, we take into account the sources and sinks: the sink term $\alpha\rho$ is weighted by the edge density $|h_x|$ and the deposition F is taken to be uniform. These results combine to give Eq. (5).

5. Validation of the continuum model

In this section we make direct comparisons between ADS simulations (3) and analytic solutions to the continuum model (5).

We begin by considering the case of periodic boundary conditions: $\rho_0 = \rho_n$ and $\rho_1 = \rho_{n+1}$, which lead to an n-periodic, steadily moving step-train on the microscale. One would expect this solution to emerge on any long step train with nearly uniform spacing. The time-averaged adatom densities at step edges $\rho \equiv \langle \rho_1^j \rangle$ is uniform in this case so that there is no density-gradient-driven surface current, but, as explained earlier, there is a surface current due to the ES barrier and this current is potentially enhanced by non-equilibrium effects.

The solution to the continuum model has a mean current satisfying $J = S\rho h_x$ for a periodic adatom distribution. From Eq. (5) we see that a steady solution will satisfy

$$h_t = F = \alpha\rho|h_x| \tag{13}$$

which has the microscale interpretation (10), and, for steps moving to the right, yields the relationship

$$-J = -S\rho_1 h_x = \frac{SF}{\alpha}. \tag{14}$$

Thus, for these especially simple boundary conditions our equations predict a surface current that is linear in F with a slope that depends only on the hopping rates at leading order.

In Fig. 5a and b, we compare the value of S given by Eq. (11) to a value calculated from Eq. (14) and a current $\bar{J}_i$ that is computed via ADS (3). The variation in these two values is shown as a function of α, k_n^+; in each case the remaining parameters are held fixed. In both cases the agreement is seen to be very good, suggesting that the drift term has been expressed correctly.

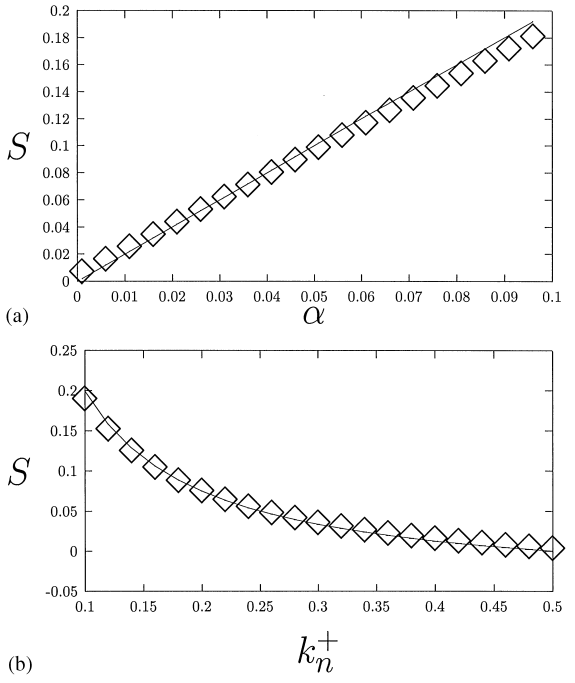

Fig. 5. A comparison of the value of S given by Eq. (11) to a value calculated from Eq. (14) and a current $\bar{J}_i$ that is computed via the rate equations (3). The variation in these two values is shown as a function of α and k_n^+; in each case the remaining parameters are held fixed.

While periodic boundary conditions have the merit of isolating the effects of the ES-barrier-induced drift, the uniform adatom density ρ eliminates the dependence of the solution upon D. To explore the combined effects of the diffusion and drift terms we examine the case of fixed-flux boundary conditions: $J_1 = J_N = J$, where N is the width of the entire domain measured in lattice sites. A steady solution, when it exists, will still adhere to Eq. (10), with $\rho = \langle \rho_1 \rangle$ varying on the macroscopic length scale. Eq. (5) reduces to

$$D\rho_x - S\rho h_x = -J.$$

When the boundary condition is $J = 0$, the uphill drift produced by the ES barrier is exactly balanced by a downward flux due to a gradient in the adatom density. Eliminating h_x via Eq. (13)

reduces this to

$$D\rho_x - \frac{SF}{\alpha} = -J \tag{15}$$

indicating a linear adatom density

$$\rho = \frac{n_0 F}{\alpha} - \left(\frac{FS}{\alpha D} - \frac{J}{D}\right)x, \tag{16}$$

where n_0 is the width of the left-most step which is enforced as a boundary condition on $h_x(0)$. The corresponding solution for the height is

$$h(x) = \frac{FD}{\alpha J - SF}\log\left(\frac{n_0 DF + (\alpha J - SF)x}{n_0 DF + (\alpha J - SF)N}\right), \tag{17}$$

where N is the width of the entire step train.

Fig. 6, which plots adatom density as a function of lattice site for a 200- and 400-site lattice when there is no imposed current J, shows that this linear solution appears to hold when the width of the step train is sufficiently small, but not when it becomes long. Even in the first figure, there are small regions near the ends of the step train where the linear solution breaks down. In the case of the longer step train, the adatom density becomes too small and the steps too bunched for our model to hold; indeed Eq. (15) predicts a negative adatom density if the step train is longer than Dn_0/S. In this situation, one finds that the numerical solutions to the difference equations do not converge to a steady state in the region beyond this critical length.

Thus quantitative comparisons for fixed-flux solutions are complicated by the competing constraints of large finite-domain-size effects for small step trains and the breakdown of the steady solution for large step trains. Nevertheless, in Figs. 7 and 8 we have superimposed the analytic solutions for the height onto solutions from simulations for several values of the parameters. In Fig. 7, the ES barrier is zero (i.e. $k_n^+ = k_s$) and the imposed current J is varied from $-F$ to F. The curvature of the step train is accurately predicted, the top figure being concave down and the lower figure being concave up. The variation from a linear step train can be made stronger by increasing the imposed current J. If this is done, the quantitative agreement between the simulated and analytic solutions decreases, as there are presently no terms in the continuum model (5) that would account for the curvature of the step train. One could presumably capture these effects by considering slowly varying step trains, in which case one would anticipate terms involving h_{xx} to appear in the continuum model.

In Figs. 8a–c, the central figure has an imposed current J chosen to balance the effects of the ES barrier (which is nonzero for this sequence of figures). The first and third figures have imposed

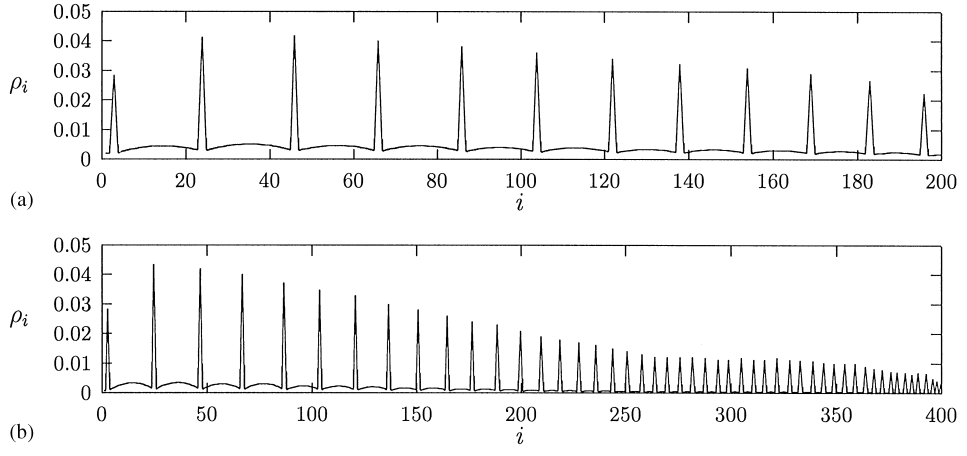

Fig. 6. (a) The quasi-equilibrium adatom density for a 200-site lattice and (b) for a 400-site lattice, all other parameters being equal. Ignoring end effects the first of these is well-approximated by a linear function; the second is linear up until around the 250th lattice site.

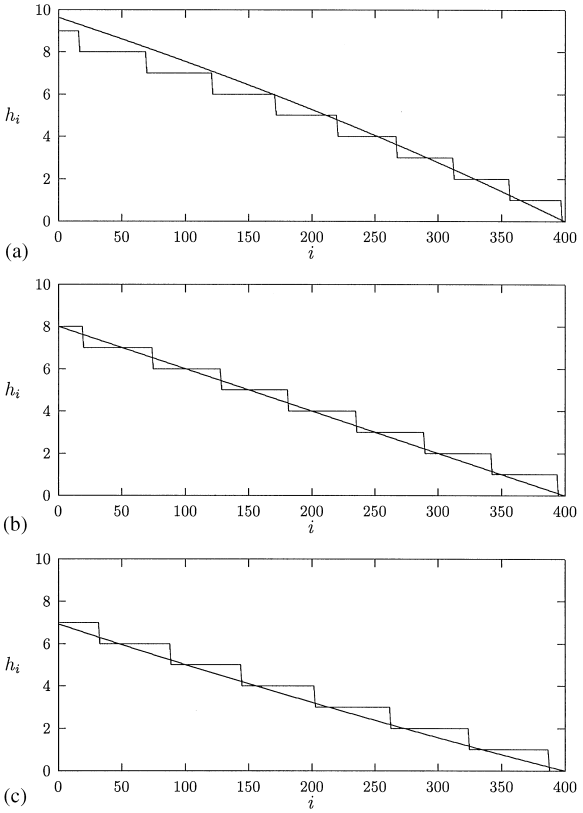

Fig. 7. The surface profile $h(x)$ for imposed surface currents $J = F$, $J = 0$ and $J = -F$. The smooth curve corresponds to the analytic solution (17); the stepped curve is the result of simulation.

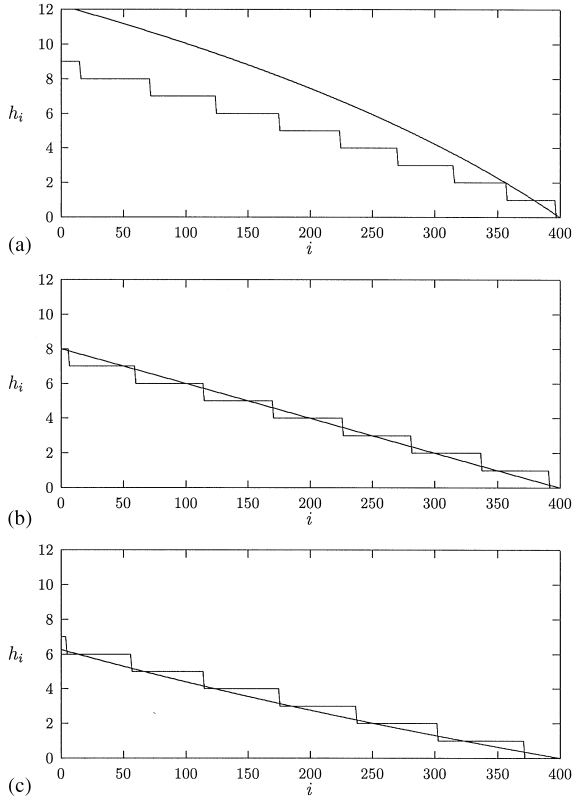

Fig. 8. The surface profile $h(x)$ for an imposed surface current $J = 0$, $3F/4$ and $3F/2$. The smooth curve corresponds to the analytic solution (17); the stepped curve is the result of simulation. For the chosen parameter values, the imposed current $J = 3F/4$ should balance the ES-barrier-induced drift, producing a linear surface.

currents that slightly over and under-compensate for the inherent drift due to the ES barrier. The first figure provides an example of how the present theory over-predicts the departure from a linear step train when curvatures are large.

6. Extension to 2 + 1 dimension and multi-species growth

Replacing the spatial derivative in Eq. (5) with a gradient operator, suggests the 2 + 1 dimensional analog

$$\bar{\rho}_t = D\nabla^2\rho - S\nabla(\rho\nabla h) - \alpha\rho|\nabla h| + F, \tag{18}$$

$$h_t = \alpha\rho|\nabla h|, \tag{19}$$

where $\bar{\rho}$ and ρ are related by a result analogous to Eq. (12).

The principal advantage of this model is its ability to move beyond single-component crystals. In the multi-species setting, there is an analog to Eq. (18) for each relevant species, which may include a variety of intermediate species as well as the materials that are eventually incorporated into the crystal. The resulting system of reaction–diffusion equations is coupled to a generalized form of Eq. (19)

$$\rho_t^i = D^i\nabla^2\rho^i - S^i\nabla(\rho^i\nabla h) + \mathscr{S}^i - \mathscr{E}^i|\nabla h| + \mathscr{F}^i, \tag{20}$$

$$h_t = \tilde{\mathscr{E}}|\nabla h| + \tilde{\mathscr{S}}. \tag{21}$$

The terms $\mathscr{F}^i$, $\mathscr{S}^i$ and $\mathscr{E}^i$ represent the flux of each species onto the substrate, terms due to surface reactions and terms due to edge reactions; the latter two are made more explicit below. Note that the species arriving onto the film/substrate may not be the same species incorporated into the film. For example, in metal-organic CVD, metallic compounds are carried to the surface attached to highly volatile organic precursors, which may decompose at or near the film surface, depending on temperature conditions.

We have made the assumption that the number density of each species is much smaller than the density of available lattice sites, which represent temporary resting points for a diffusing adatom. This allows us to use diffusion coefficients D^i that are characteristic of the behavior of each species measured independently of the others and avoids complicated cross-diffusion effects. This is a realistic assumption for most growth processes.

Unlike the single species case, the sink and source terms must now be distinguished. Surface reactions, including surface-building reactions (nucleation), surface decomposition and the formation of intermediate species are represented by

$$\mathscr{S}^i = \sum_j K_{ij} \prod_k [\rho^k]^{G_{ikj}}, \quad \tilde{\mathscr{S}} = \sum_{i,j} \tilde{K}_{ij} \prod_k [\rho_k]^{G_{ikj}},$$

where the exponents G_{ikj} are determined via stoichiometry and K_{ij} are pairwise reaction rates. Similarly, the edge-building reactions take the form

$$\mathscr{E}^i = \sum_j k_{ij} \prod_k [\rho^k]^{\gamma_{ikj}}, \quad \tilde{\mathscr{E}} = \sum_j \tilde{k}_{ij} \prod_k [\rho^k]^{\gamma_{ikj}}.$$

A general surface model can contain an overwhelming number of undetermined parameters, with no practical means of measuring most of them. Ultimately, this necessitates the development of reduced models that rely on simplifications, such as rate-determining reactions.

7. Summary

In this paper, we have proposed a new model for epitaxial film growth appropriate for the step-flow regime. The model is in many respects a hybrid between the existing continuum models of the BCF-type and those using height evolution equations. The principal features of the model are that it is readily extended to multi-species systems, it can be applied over large length scales and that the coefficients can be expressed in terms of parameters used in KMC simulations, allowing quantitative comparisons to be made. For comparison purposes we introduced – but will discuss at length elsewhere – a new simulation tool, the atomistic difference scheme (ADS), that serves as a fast version of KMC simulations. Comparisons between ADS and analytic solutions to the single-species version of our continuum model were seen to agree.

The model is readily extended in many different ways. With an appropriate nucleation model one can use these equations to simulate island-growth mode. While we have assumed a uniform deposition of adatoms, there is no reason this could not be stochastically driven or coupled to a deposition process like chemical vapor deposition. Indeed, both of these extensions are actively being pursued. One of the principal aims of this formulation is to extend its application to surface chemistry and other multi-species effects. In this framework one can separately account for bulk surface reactions, reactions which are coupled to the edge density and reactions involving precursors or intermediate species. Modifications specific to a $2+1$ dimensional version of this model include the incorporation of kink densities and anisotropic growth effects. One anticipates that when all of the various types of step-edge interactions are properly accounted for, Eq. (20) will naturally take on a four-fold anisotropy for the case of cube-on-cube epitaxy. Finally, the potential ϕ which determines the hopping rates could be coupled to equations that model the large-scale elastic behavior of the crystal.

Acknowledgements

The authors would like to thank Professor Robert V. Kohn of New York University and Aaron Yip of Purdue University for many helpful

discussions that improved this work. We would also like to thank NSF and DARPA for providing funding for this research through the VIP program.

References

[1] W.K. Burton, N. Cabrera, F.C. Frank, Philos. Trans. Roy. Soc. London 243A (1951) 299.
[2] D.D. Vvedensky, A. Zangwill, D.N. Luse, M.R. Wilby, Phys. Rev. E 48 (1993) 852.
[3] R. Ghez, S.S. Iyer, IBM J. Res. Dev. 32 (1988) 804.
[4] R.E. Caflisch, M.F. Gyure, B. Merriman, C. Ratsch, Phys. Rev. E. 59 (1999) 6879.
[5] M. Kardar, G. Parisi, Y.-C. Zhang, Phys. Rev. Lett. 56 (1986) 889.
[6] R.E. Caflisch, M.F. Gyure, B. Merriman, S.J. Osher, C. Ratsch, D.D. Vvedensky, J.J. Zinck, Appl. Math. Lett. 12 (1999) 13.
[7] M.F. Gyure, C. Ratsch, B. Merriman, R.E. Caflisch, S.J. Osher, J.J. Zinck, D.D. Vvedensky, Phys. Rev. E 58 (1999) 6927.
[8] P. Smereka, Physica D 138 (2000) 282.
[9] P. Smilauer, D.D. Vvedensky, Phys. Rev. B 52 (1995) 14 263.
[10] W.E., N.K. Yip, J. Stat. Phys., submitted for publication.
[11] J.D. Weeks, G.H. Gilmer, Adv. Chem. Phys. 40 (1979) 157.
[12] R.L. Schwoebel, J. Appl. Phys. 40 (1969) 614.
[13] I. Elkinani, J. Villain, J. Phys. I 4 (1994) 949.
[14] P. Politi, J. Villain, Phys. Rev. B 54 (1996) 5114.